HHS Public Access

Author manuscript

Nat Neurosci. Author manuscript; available in PMC 2016 June 02.

Published in final edited form as:

Nat Neurosci. 2016 February ; 19(2): 220–222. doi:10.1038/nn.4199.

The indirect pathway of the nucleus accumbens shell amplifies neuropathic pain

Wenjie Ren[1], **Maria Virginia Centeno**[1], **Sara Berger**[1], **Ying Wu**[2], **Xiaodong Na**[2], **Xianguo Liu**[2], **Jyothisri Kondapalli**[1], **A Vania Apkarian**[1,3], **Marco Martina**[1,3], and **D James Surmeier**[1,3]

[1]Department of Physiology, Feinberg School of Medicine, Northwestern University, Chicago, Illinois, USA

[2]Pain Research Center and Department of Physiology, Zhongshan School of Medicine, Sun Yat-Sen University, Guangzhou, China

Abstract

We examined adaptations in nucleus accumbens (NAc) neurons in mouse and rat peripheral nerve injury models of neuropathic pain. Injury selectively increased excitability of NAc shell indirect pathway spiny projection neurons (iSPNs) and altered their synaptic connectivity. Moreover, injury-induced tactile allodynia was reversed by inhibiting and exacerbated by exciting iSPNs, indicating that they not only participated in the central representation of pain, but gated activity in ascending nociceptive pathways.

Forebrain limbic circuits have long been hypothesized to be critical for the representation of pain[1–4]. The medial shell of the NAc (msNAc) is a key node in this circuitry, integrating signals from mesencephalic dopaminergic neurons, as well as neurons residing in the ventral hippocampus, amygdala and frontal cortices, all of which are structures that process affective information[5,6]. Human imaging studies suggest that this convergence in the NAc is important in both acute and chronic pain states[7,8]. The NAc shell appears to be particularly important in evaluating impending pain[8]. Indeed, inactivating the msNAc with lidocaine[9] or infusing a DA agonist[10] diminishes tactile allodynia in spared nerve injury (SNI) model of neuropathic pain.

Although intriguing, these manipulations ignore the complex circuitry of the msNAc. Unraveling how this circuitry is engaged in pain states could lead to new targeted therapeutic

Correspondence should be addressed to D.J.S. (; Email: j-surmeier@northwestern.edu)

[3]These authors contributed equally to this work.

Note: Any Supplementary Information and Source Data files are available in the online version of the paper.

AUTHOR CONTRIBUTIONS

W.R. performed the electrophysiological recordings, morphological reconstruction, data analysis and drafted the manuscript. M.V.C. performed surgeries, behavioral testing and analysis. S.B. performed behavioral testing and analysis. Y.W. and X.N. performed surgeries, western blot analysis and microdialysis. X.L. designed and supervised western blot and microdialysis experiments. J.K. generated the AAV virus for stereotaxic injections. D.J.S., A.V.A. and M.M. conceived of and designed the project, supervised the experiments and drafted the manuscript.

COMPETING FINANCIAL INTERESTS

The authors declare no competing financial interests.

strategies that lack adverse side effects. The msNAc has two parallel, opposing networks charged with affective evaluation of salient events that shape behavior[11,12]. The direct pathway, which is linked to reward and positive affect, is anchored by GABAergic direct spiny projection neurons (dSPNs) whose activity is enhanced by dopamine (DA) acting at postsynaptic D1 DA receptors. The indirect pathway, which is linked to aversive events and negative affect, is anchored by GABAergic indirect spiny projection neurons (iSPNs) whose activity is suppressed by DA acting at postsynaptic D2 DA receptors[11,12].

How these two networks respond to neuropathic pain is largely unknown. To begin filling this gap, we subjected transgenic mice expressing a red reporter in dSPNs and a green reporter in iSPNs (Fig. 1a) to an SNI protocol and then examined them 5 d later when mice exhibited a pronounced tactile allodynia (Supplementary Fig. 1a). The intrinsic excitability, dendritic morphology and excitatory synaptic connectivity of msNAc dSPNs was not altered in SNI mice (Supplementary Figs. 2 and 3c–e). In contrast, the intrinsic excitability of both ipsilateral and contralateral iSPNs was substantially elevated in SNI mice (Fig. 1b, c and Supplementary Fig. 3a, b).

This shift was attributable to two adaptations. First, iSPNs in SNI mice had fewer and shorter dendrites (Fig. 1d, e and Supplementary Fig. 4a, b). Other dendritic features were unchanged (Supplementary Fig. 4d, e). Dendritic paring was accompanied by increased input resistance, lower rheobase current (Supplementary Fig. 3d, e) and lower miniature excitatory postsynaptic current (mEPSC) frequency, but not amplitude (Fig. 1f, g and Supplementary Fig. 4c). Second, extracellular DA in NAc, which inhibits iSPNs[13], was lower in SNI rats (Fig. 1h); consistent with the inference that there was an alteration in ambient DA signaling, the D2 receptor antagonist sulpiride (5 μM) increased the excitability of iSPNs from unlesioned mice, but not those from SNI mice (Supplementary Fig. 5). This drop was attributable to a reduction in the spontaneous spiking of ventral tegmental area (VTA) dopaminergic neurons projecting to the msNAc in VTA slices from SNI mice (Fig. 1i, j) and increased NAc DA transporter (DAT) expression in SNI rats (Supplementary Fig. 6a, f). Indeed, application of the DAT antagonists bicifadine (20 μM) or GBR12909 (20 μM) partially restored iSPN excitability in tissue from SNI mice (Supplementary Fig. 6b–e).

Because the adaptations in iSPNs appeared to stem from a hypodopaminergic state, an attempt was made in mice and rats to reverse them by combining systemic administration of L-3,4-dihydroxyphenylalanine (L-DOPA), a precursor of DA that is well tolerated by humans and gets across the blood-brain barrier, and the non-steroidal anti-inflammatory naproxen. Administration of both L-DOPA (0.3 mg per kg of body weight) and naproxen (30 mg per kg) was started 2 h before nerve lesion and continued for 5 d. The combination prevented the physiological and anatomical adaptations seen in iSPNs from SNI mice (Fig. 2a–f and Supplementary Fig. 7a). Moreover, combined treatment (but not either alone[14–16]) blocked the development of tactile allodynia in SNI mice and rats (Fig. 2g and Supplementary Fig. 7b). Combined treatment also blunted deficits in social recognition that accompany SNI rats (Supplementary Fig. 7d–f). This treatment effect generalized to an inflammatory pain model created by injecting carrageenan in rats' hindpaws, where combined (but not individual) treatment rapidly and completely abolished tactile allodynia (Supplementary Fig. 7c). The inability of systemic L-DOPA administration alone to affect

pain behavior might be because of its limited ability to elevate dopamine concentration, particularly in the face of increased levels of NAc DAT[17]. To overcome this shortcoming and to provide a more direct test of D2 receptor involvement in neuropathic pain, we administered the D2/3 receptor agonist pramipexole, which has good brain bioavailability[18], systemically in rats before SNI. Pramipexole alone (0.3 mg per kg) significantly blunted SNI-induced tactile allodynia (U = 2, $P = 0.0087$; Fig. 2h).

The most parsimonious interpretation of the drop in glutamatergic mEPSC frequency was that there was a reduction in the number of excitatory, glutamatergic synapses on iSPNs. To test this hypothesis, we used optogenetic approaches to examine the two major glutamatergic afferents to NAc shell SPNs[6], neurons in the infralimbic medial prefrontal cortex (IL; Fig. 3a) and the ventral hippocampus (vHipp; Fig. 3b), in *ex vivo* brain slices from SNI and control mice (Supplementary Fig. 8a). The ratio of the AMPA receptor (AMPAR)-mediated EPSC and the NMDA receptor (NMDAR)-mediated EPSC was estimated to gauge changes in synaptic strength[6]. As predicted, the IL-evoked AMPAR/NMDAR ratio in iSPNs from SNI mice was significantly reduced (U = 2, $P = 0.0087$; Fig. 3c, d), whereas it was unchanged in neighboring dSPNs (Supplementary Fig. 8b, c). Unexpectedly, at the same time point following SNI, the vHipp-evoked AMPAR/NMDAR ratio was significantly greater in msNAc iSPNs (U = 3, $P = 0.0152$; Fig. 3e, f), whereas it was unchanged in neighboring dSPNs (Supplementary Fig. 8d, e). These results are consistent with the proposition that the aggregate strength (number and/or function) of IL-iSPN synapses was reduced following SNI, but that of vHipp-iSPN synapses was increased.

Recent work has shown that, in the NAc core, SNI triggers an upregulation in GluN2B subunits in NMDARs, resulting in long-term depression of excitatory synapses on iSPNs[4]. A hallmark of this shift in subunit composition is a slowing of NMDAR decay kinetics[19]. In agreement with this earlier work, the decay of the NMDAR EPSC was slowed at IL-iSPN synapses, but not at IL-dSPN synapses in msNAc (Supplementary Fig. 8f, g). However, at the vHipp synapses, which appeared to be strengthened, there was no change in NMDAR EPSC decay rate (Supplementary Fig. 8h, i).

Although these results establish a compelling correlation between pain behavior and activity in msNAc iSPNs, they do not prove that iSPN activity was responsible for tactile allodynia. To determine whether there was a causal linkage, we activated msNAc iSPNs *in vivo* using a chemogenetic approach, allowing bidirectional control of iSPN excitability *in vivo*[20]. After verifying bidirectional control of iSPNs in *ex vivo* brain slices (Supplementary Fig. 9), we administered the designer ligand ($PSAM^{89S}$) to chemogenetically alter SNI mice and controls. Chemogenetically exciting iSPNs worsened tactile allodynia 5 d after SNI, whereas inhibiting iSPNs alleviated allodynia (Fig. 3g). These results establish a clear causal connection between the activity in msNAc iSPNs and tactile allodynia.

There are several important conclusions from these results (Supplementary Fig. 10b). First, following peripheral nerve injury, there is a cell-specific upregulation in msNAc iSPN excitability that worsens tactile allodynia. The ability of msNAc iSPNs to drive descending pathways that control the reactivity of segmental withdrawal circuitry is consistent with a number of previous studies implicating the VTA, D2 DA receptors and the NAc in tactile

allodynia[9,10,15] and aversion[12]. Second, the adaptations in msNAc iSPNs underlying the worsening of allodynia can be blunted either with L-DOPA in combination with naproxen or pramipexole, a D2/3 dopamine receptor agonist with good brain availability[18]. Not only do these results shed new light on the specific fore-brain circuits involved in neuropathic pain, they point to a new therapeutic approach for managing or preventing its development in humans.

ONLINE METHODS

Animals

All electrophysiological and morphological studies were carried out in 8-week-old male C57BL6 bacterial artificial chromosome (BAC)-transgenic mice (D1 receptor-Td Tomato and D2 receptor–enhanced green fluorescent protein [eGFP]) or PSAM virus injected 8-week-old male A2A::Cre mice (Supplementary Fig. 9). 8-week-old male A2A::Cre mice were used in the chemogenetic studies of *in vivo* modulating iSPNs by PSAM virus injection (Fig. 3g). Animals were group-housed with littermates, with food and water available ad libitum and with a 12-h light/dark cycle (7 A.M.–7 P.M.). Tactile threshold of each animal was measured one day pre-surgery and on assigned dates post-surgery. In another set of behavioral experiments, the effects of oral drug treatment on tactile sensitivity were assessed on 8-week-old male BAC mice (Fig. 2g) and 8-week-old male Sprague-Dawley rats (Fig. 2h and Supplementary Fig. 7b, c); 8-week-old female and male Sprague-Dawley rats were used in the sociability test (Supplementary Fig. 7d–f). In these groups of animals, tactile thresholds and sociability were measured before surgical manipulation and then again after surgery. 8-week-old male Sprague–Dawley rats were also used for *in vivo* brain microdialysis and DAT quantification using western blot experiments. Rats were group-housed as above. All studies were approved by the Animal Care and Use Committee of Northwestern University or by the Local Animal Care Committee (Sun Yat-sen University) and were carried out in accordance with the guidelines of the National Institutes of Health on animal care and with the ethical guidelines for investigation of experimental pain in conscious animals[21].

Neuropathic pain model: SNI

The SNI model has been described previously[22]. Mice and rats were anesthetized with isoflurane 1.5–2.5% (vol/vol) and a mixture of 30% N_2O and 70% O_2. The left hind leg sciatic nerve was exposed at the level of the trifurcation into the sural, tibial, and common peroneal nerves. The tibial and common peroneal nerves were tightly ligated and severed, leaving the sural nerve intact. Animals in the Sham surgery group had their sciatic nerve exposed as in the SNI procedure, but they received no further manipulations.

Tactile sensitivity

Paw withdrawal thresholds to Von Frey filament stimulation (VF) were used to assess mechanical sensitivity of the hind-paws. Animals were placed in a Plexiglas box with a wire grid floor and allowed to habituate for 10–15 min (rats) or 45 min to 1 h (mice). Then, filaments of various forces (Stoelting) were applied to the plantar surface of each hind-paw. Filaments were applied in a descending and ascending pattern, determined by the response

of the animal. Each filament was applied for a maximum of 2 s, and paw withdrawal in response to the filament was considered a positive response. 50% thresholds were calculated as described previously[23]. The injured paw withdrawal thresholds of all SNI animals were substantially decreased compared with the pre-surgery level and Sham animals (Supplementary Fig. 1a).

Electrophysiology

Brain slices preparation—Sagittal/coronal brain slices of the msNAc (Supplementary Fig. 1b) or VTA (250 μm) were obtained from BAC D1 and D2 receptor transgenic mice or PSAM virus injected A2A::Cre mice. The mice were anesthetized with ketamine/xylazine and perfused transcardially with ice-cold artificial CSF (aCSF), containing in mM: 125 NaCl, 2.5 KCl, 1.25 NaH_2PO_4, 2.0 $CaCl_2$, 1.0 $MgCl_2$, 25 $NaHCO_3$, and 25 glucose, saturated with 95% O_2 and 5% CO_2. Brains were rapidly removed and sliced in oxygenated, ice-cold, aCSF using a VT1200S vibratome (Leica Microsystems). Sagittal NAc medial shell slices did not contain any dorsal striatal tissue (0.44–0.52 mm lateral); they were transferred to a holding chamber and incubated in aCSF at 35 °C for 30 min, and then stored at room temperature until used for patch clamp recordings (1–5 h). The extracellular aCSF was saturated with 95% O_2/5% CO_2 at all times to maintain oxygenation and a pH ~7.4.

Visualized whole-cell patch-clamp recording ex vivo—Slices were visualized using an upright microscope (Nikon) equipped with infrared differential interference contrast (IR-DIC) optics and with a Hitachi CCD camera (KP-M2RN). The recording chamber was superfused with carbogen-saturated aCSF at a flow rate of 2–3 ml min^{-1}. Picrotoxin (100 μM) was added to block $GABA_A$ receptor– mediated IPSCs. A combination of CNQX (10 μM) and D-AP5 (50 μM) was used to block glutamatergic transmission during action potential recording. Recordings were made at 32–34 °C using a Multiclamp 700B amplifier with pClamp 10.3 software (Molecular Devices). Signals were filtered at 5 Hz (current clamp) or 2 Hz (voltage clamp) and digitized at 10 kHz with a Digidata 1322A (Molecular Devices). Patch electrodes were pulled on a Flaming-Brown horizontal puller (P-97; Sutter Instruments) from filamented, thick-wall borosilicate-glass (1.5-mm O.D., Sutter Instruments). Pipette resistance was typically ~3–5 MΩ when filled with an internal solution consisting of: 140 mM $KMeSO_4$, 10 mM KCl, 10 mM HEPES, 2 mM Mg_2ATP, 0.4 mM NaGTP, 10 mM sodium phosphocreatine and 0.2% (wt/vol) biocytin; pH 7.25–7.30; 300 mOsm.

In each NAc shell slice, neuronal somatic eGFP or Td-Tomato expression was verified routinely in cell-attach to confirm cell identity before breaking into whole-cell mode. Current clamp recordings were performed to quantify firing properties. Spikes were evoked using current step injections (800-ms duration at 0.1 Hz, −160 to +320 pA range with 20-pA steps). There is no detectable difference in intrinsic excitability of either iSPNs or dSPNs between sham and naive BAC transgenic animals (Supplementary Fig. 1c, d). Rheobase current was defined as the first current step capable of eliciting an action potential. Input resistance (Ri) was monitored on-line with a 40-pA, 150-ms current injections and only cells with a stable Ri (≤20% change for the duration of the recording) were further analyzed. Basal firing frequency of medial VTA neurons was measured over a 5-min current-clamp

recording and the amplifier bridge circuit were adjusted to compensate for electrode resistance and monitored. mEPSCs were measured in voltage clamp at a holding potential of −80 mV and in the presence of 500 nM tetrodotoxin (TTX, to block voltage-gated sodium currents). Frequency and amplitude distributions of mEPSCs were analyzed using MiniAnalysis program 6.0.3 (Synaptosoft) over a 5-min interval.

Optically evoked synaptic responses—EPSCs of msNAc SPNs were evoked by ChR2 stimulation using 473-nm wavelength light pulses (1 ms, 0.33-Hz LED, CoolLED), and were recorded in voltage clamp (V_h = −80 mV). The access resistance was monitored by a hyperpolarizing step of −14 mV with each sweep. For recordings designed to determine the AMPA receptor/NMDA receptors current ratios, the internal solution contained 3 mM QX-314 and cells were held at +40 mV. AMPAR-mediated currents were isolated with the selective NMDAR antagonist AP5 (50 μM). The NMDAR-mediated current was then digitally obtained by taking the difference current before and after AP5 application. NMDAR EPSC decays were fitted (t = 0 at the peak) with a two-exponential decay function (in Graphpad Prism), and the weighted decay (τ_w) was calculated according to: $\tau_w = (\tau_1 * a_1) + (\tau_2 * a_2)$, where a_1 and a_2 are the relative amplitudes of the two exponential components.

Drugs and drug application—Sulpiride and Bicifadine were obtained from Tocris. CBR12909 was obtained from Sigma-Aldrich. PSEM^{89s} was obtained from S.M. Sternson (Howard Hughes Medical Institute) and Apex Scientific. Drugs were bath applied for at least 15 min to establish equilibrium in the tissue.

Confocal imaging and anatomical reconstruction

For anatomical reconstruction, 0.2% biocytin (wt/vol) was included in the internal solution and neurons were recorded in whole-cell mode for at least 30 min. Slices were fixed in 4% paraformaldehyde (wt/vol) overnight. After several washes, slices were reacted for 6 h with streptavidin-Cy5 (1:200, Invitrogen, catalog number: SA1011) in 0.5% Triton-X (vol/vol), 1% BSA (wt/vol), 10% normal goat serum (vol/vol) (in PBS) at 20–22 °C in the dark. Sections were then washed and coverslipped with prolong gold antifade reagent (Invitrogen). A cell was rejected if the soma was not intact or any dye was seen in neighboring cells. For anatomical reconstruction, serial optical sections (Z stacks) were acquired using a 0.415 × 0.415 × 0.5 μm^3 voxel size on a laser-scanning confocal microscope (LSM 510; Olympus) with a 60×/1 NA oil-immersion objective (Zeiss). Z-series of the same cell were combined using Fiji Software (VIAS, Mt. Sinai Computational Neurobiology and Imaging Center), and subsequently reconstructed and analyzed using the Neurolucida/Neuroexplorer suite (MicroBrightField). No correction was applied for tissue shrinkage. For spine counting, serial Z-stacks were acquired using a 0.069 × 0.069 × 0.1-μm^3 voxel size. Images were deconvoluted using Autoquata (MediaCybernetics). Counting was performed on 45–105-μm long segments of the principal dendrite. Spines were counted only if they had both a punctuate head and visible neck.

In vivo brain microdialysis

Under chloral hydrate anesthesia (0.4 g per kg, i.p.), rats were implanted bilaterally in the NAc (AP +1.7 mm; ML ± 0.8 mm; DV −7 mm) with dialysis guide cannulas (10 mm, MD-2250, O-ring, BASi). The guide cannulas were fixed to the skull with stainless steel screws and dental acrylic. *In vivo* brain microdialysis was performed in freely moving rats at assigned time points to examine the concentration of dopamine (DA) in NAc. The 320-μm diameter dialysis probes, which have 2-mm-long functional membranes, were inserted into the NAc 1 d before the experiment to minimize damage-induced dopamine release. On the day of the experiment, dialysis buffer (124 mM NaCl, 3.3 mM KCl, 1.2 mM KH_2PO_4, 26 mM $NaHCO_3$, 2.5 mM $CaCl_2$ and 2.4 mM $MgSO_4$, pH 7.4) was perfused through the dialysis probe (1 μl min^{-1}) via syringe pump (MD-1001, BASi) for 90 min before sample collection. In the next 1 h, 10-μl dialysis samples were collected every 30 min and dialysate DA was immediately measured by HPLC with electrochemical detection system (BASi). DA was separated using a BASi C18 column (5 μm, 100 mm × 1 mm) and oxidized/reduced using a BASi LC Epsilon electrochemical detector which contained a BASi 6 mm Glassy carbon electrode and three silver/silver chloride reference electrodes (MF-2078, BASi). The DA mobile phase consists of 3.28 mM sodium heptanesulfonate, 0.16 mM EDTA, 100.81 mM sodium acetate, and 93 mM citric acid, PH 3.7. The area under the curve of the DA peak was measured using BASi ChromGraph Performance-Verified Software (Ver. 2.5x). DA values were quantified with an external calibration curve (50–2,000 pg ml^{-1}).

Western blot analysis

Animals were decapitated at assigned date post-surgery, and the brains were removed and sliced. NAc tissue was homogenized and equal amounts of proteins were separated by gel electrophoresis (SDS-PAGE) and transferred to PVDF membrane. The membrane was blocked and then probed with primary antibody against DAT (1:200, Millipore, catalog number: MAB369) and β-actin (1:1,000, Cell Signaling Technology, catalog number: 4967) overnight at 4 °C. Membranes were then incubated with an HRP-conjugated secondary antibody (CST) at room temperature. Protein bands were detected by ECL detection reagent (RPN2232; GE Healthcare) and captured on an autoradiography film (Kodak). Integrated optical density was determined using Image-Pro Plus software 6.0 (Media Cybernetics). Standard curves were constructed to verify that we operated within the linear range of the detection method.

Systemic drug administration

All the drugs were dissolved in saline and were administered at the following doses: saline (2 ml kg^{-1}), naproxen (30 mg per kg), levodopa (1.5 mg per kg), or a combination of either levodopa with naproxen or levodopa with naproxen and carbidopa (0.375 mg per kg), pramipexole (0.2 mg per kg). Individual drug doses did not change regardless of whether they were administered alone or in combination. All the drugs were obtained from Sigma-Aldrich. Drugs were given by gavage twice daily and 8 h apart during the daytime. The drug treatment began 2 h before the surgery (sham/SNI) or carrageenan injection and continued for 5 d. VF threshold measurements were taken once or twice before surgery or carrageenan injection as baseline to track the effects of the medication on pain behavior.

Sociability test

The Sociability test, adapted from ref. [24], assessed an animal's preference for social versus non-social interaction. Briefly, the apparatus consisted of an opaque Plexiglas box with two wired cups (A and B) placed directly across from one another; these cups allowed the experimental animals to approach and interact with confined conspecifics/objects without direct contact. The box was placed in a quiet room, and a camera was fixed over the box to record behavior. The animals received 10-min habituation (both cups were empty) and 24 h later, another 10-min habituation was received. Sociability test was performed after another 5-min home cage stay. In each test, a male rat was placed in the box and exposed to a juvenile female rat (Cup A) and an object (Cup B) for 10 min. The object used was approximately the same size and the same color as the conspecific to control for any different visual cues. Using ANY-maze (version 4.98) visual tracking software, we measured the time rats spent interacting with each cup (interaction is defined as rat's head being within the zone surrounding each cup), and the ratio of exploration time for Cup A over that for Cup B was calculated (Supplementary Fig. 7d). The box, cups and objects were cleaned with soapy water and wiped with bleach and alcohol before each animal's tests. Adult Sprague-Dawley rats were used and four groups were compared: sham with saline (2 ml kg^{-1}) treatment, sham with levodopa (1.5 mg per kg) and naproxen (30 mg per kg) co-administration treatment, SNI with saline treatment, and SNI with levodopa and naproxen combined treatment. Drugs were administered by gavage twice daily, which began in the morning of surgery and were continued until testing day (day 5 post surgery).

Stereotaxic injection of AAV-ChR2

For ChR2-AAV virus injection, BAC transgenic mice were anesthetized with isoflurane and the stereotaxic guided surgeries were performed. A glass filled with viral solution was lowered through a small hole drilled through the skull and two unilateral injections were made. The injection pipette was withdrawn 5 min after the infusion and the scalp was then sealed. AAV9-CAG-hChR2-mCherry-WPRE.SV40 (title: 5.16×10^{12} genoic copies per ml) were injected into imfralimbic prefrontal cortex (100 nl ChR2-AAV at coordinate of bregma 1.90, lateral 0.25, ventral 2.85) or ventral hippocampus (350 nl ChR2-AAV at coordinate of bregma −3.5, lateral 2.75, ventral 4.75). Animals were used at 3 weeks after injection and the injection site was verified *post hoc*.

In vivo activation or inhibition of NAc shell iSPNs

A2A::Cre mice were used and stereotaxic guided surgeries were performed as same as the injection of AAV-ChR2. AAV9-Syn-DIO-*rev*-$PSAM^{L141F,Y115F}$-5HT3HC-IRES-GFP-WPRE (title: 2.04×10^{13} genomic copies per ml) were used to activate iSPNs, AAV9-Syn-DIO-*rev*-$PSAM^{L141F,Y115F}$-GlyR-IRES-GFP-WPRE (title: 2.10×10^{13} genomic copies per ml) were used to inhibit iSPNs and AAV9-Syn-DIO-*rev*-GFP-WPRE (title: 2.15×10^{13} genomic copies per ml) were used for control vector. 100nl of virus were injected into bilateral msNAc at coordinate of bregma 1.65, lateral 0.65, ventral 4.6. 5 weeks after PSAM-AAV virus injection, SNI or Sham surgeries were performed. On 5 d after SNI/Sham surgery, the paw withdrawal threshold was assessed at pre- and 1 h post i.p. injection of either saline or $PSEM^{89s}$ (30 mg per kg or 10 mg per kg). In Sham animal, neither excitatory

PSAM(PSAM-5HT3) nor inhibitory PSAM (PSAM-GlyR) has effect on tactile threshold (Supplementary Fig. 10a). The injection site was verified *post hoc*.

Statistics

Data analyses were done with ClampFit 9 (Molecular Devices), MiniAnalysis 6.0.3 (Synaptosoft) and GraphPad Prism 6.0 (GraphPad Software). Distribution free statistics were used for all data sets regardless of sample size and variance. Intensity-response and morphological Sholl analysis data are presented as median with shaded interquartile (quartile 1 to quartile 3). Box plots are used to represent all the other data: the central line represents the median, the edges represent the interquartile ranges, and the whiskers represent the overall distribution. Statistical analysis was performed with GraphPad Prism 6.0 (GraphPad Software) using non-parametric tests (two-tailed Mann-Whitney rank sum test or two-tailed Wilcoxon matched-pairs signed rank Test). Kolmogorov-Smirnov tests were used for cumulative distribution analysis of miniature EPSCs. Statistical tests are indicated in each figure's legend. Data collection and analysis were not performed blind to the condition of the experiments, and no randomization was used. No data points were removed from statistical analysis except specified. In all experiments no statistical methods were used to predetermine sample sizes, but sample size is similar to sample sizes routinely used in the field for similar experiments[4]. Neurons or brain slices for each experimental group were collected from at least five mice, and one or two brain slice per mouse. In behavioral test, the animal number of each group was between 5–9 animals from at least two litters. Probability threshold for statistical significance was $P < 0.05$.

A Supplementary methods checklist is available.

Supplementary Material

Refer to Web version on PubMed Central for supplementary material.

Acknowledgments

We thank the laboratory of S.M. Sternson (Howard Hughes Medical Institute) for providing technical help and chemical compound PSEM^{89S}, and H. Fields for critically reading an earlier version of the manuscript. This work was supported by US National Institutes of Health grants DE022746 (A.V.A.), NS064091 (M.M.), NS 34696 and JPB Foundation (D.J.S.), and National Natural Science Foundation of China U1201223 (X.L.).

References

1. Raz M. Perspect Biol Med. 2009; 52:555–565. [PubMed: 19855124]
2. Holden C. Science. 1979; 204:1066–1068. [PubMed: 377485]
3. Lee M, et al. J Neurosci. 2015; 35:5247–5259. [PubMed: 25834050]
4. Schwartz N, et al. Science. 2014; 345:535–542. [PubMed: 25082697]
5. Bromberg-Martin ES, Matsumoto M, Hikosaka O. Neuron. 2010; 68:815–834. [PubMed: 21144997]
6. Britt JP, et al. Neuron. 2012; 76:790–803. [PubMed: 23177963]
7. Baliki MN, Geha PY, Fields HL, Apkarian AV. Neuron. 2010; 66:149–160. [PubMed: 20399736]
8. Baliki MN, et al. J Neurosci. 2013; 33:16383–16393. [PubMed: 24107968]
9. Chang PC, et al. Pain. 2014; 155:1128–1139. [PubMed: 24607959]
10. Sarkis R, Saadé N, Atweh S, Jabbur S, Al-Amin H. Exp Neurol. 2011; 228:19–29. [PubMed: 21146525]

11. Hikida T, Kimura K, Wada N, Funabiki K, Nakanishi S. Neuron. 2010; 66:896–907. [PubMed: 20620875]
12. Danjo T, Yoshimi K, Funabiki K, Yawata S, Nakanishi S. Proc Natl Acad Sci USA. 2014; 111:6455–6460. [PubMed: 24737889]
13. Gerfen CR, Surmeier DJ. Annu Rev Neurosci. 2011; 34:441–466. [PubMed: 21469956]
14. Padi SS, Kulkarni SK. Pharmacol Biochem Behav. 2004; 79:349–358. [PubMed: 15501312]
15. Pelissier T, Laurido C, Hernandez A, Constandil L, Eschalier A. Eur J Pharmacol. 2006; 546:40–47. [PubMed: 16905131]
16. Cobacho N, De la Calle JL, González-Escalada JR, Paíno CL. Brain Res Bull. 2010; 83:304–309. [PubMed: 20813171]
17. Amara SG, Kuhar MJ. Annu Rev Neurosci. 1993; 16:73–93. [PubMed: 8096377]
18. Deleu D, Northway MG, Hanssens Y. Clin Pharmacokinet. 2002; 41:261–309. [PubMed: 11978145]
19. Sanz-Clemente A, Nicoll RA, Roche KW. Neuroscientist. 2013; 19:62–75. [PubMed: 22343826]
20. Sternson SM, Roth BL. Annu Rev Neurosci. 2014; 37:387–407. [PubMed: 25002280]
21. Zimmermann M. Pain. 1983; 16:109–110. [PubMed: 6877845]
22. Decosterd I, Woolf CJ. Pain. 2000; 87:149–158. [PubMed: 10924808]
23. Chaplan SR, Bach FW, Pogrel JW, Chung JM, Yaksh TL. J Neurosci Methods. 1994; 53:55–63. [PubMed: 7990513]
24. Yang M, et al. Front Behav Neurosci. 2007; 1:1. [PubMed: 18958184]

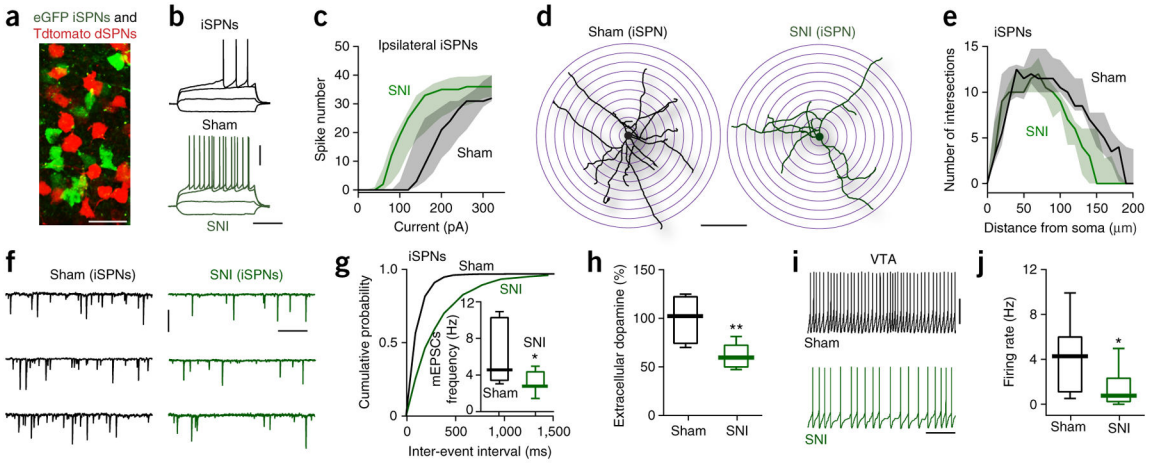

Figure 1.

SNI induced iSPNs reorganization in msNAc. (**a**) Identification of iSPNs (eGFP, green) and dSPNs (Tdtomato, red) in BAC mice. Under our recording conditions, eGFP- and Tdtomato-labeled neurons were both clearly visible in every individual msNAc slice (n = 148 slices from 70 mice). Scale bar represents 20 μm. (**b**) Representative voltage traces showing the responses of msNAc iSPNs from Sham (n = 11 neurons from 5 mice) and SNI (n = 14 neurons from 5 mice) animals to injections of depolarizing currents. Scale bars represent 30 mV and 300 ms. (**c**) Intrinsic iSPN excitability was augmented in ipsilateral msNAc slices from SNI animals (n = 5 neurons from 5 Sham mice and n = 7 neurons from 5 SNI mice, U = 3678, P = 0.0007, Mann-Whitney test). Data are shown as median with shaded interquartile (quartile 1 to quartile 3). (**d**, **e**) Three-dimensional Sholl analysis of reconstructed iSPNs revealed that SNI iSPNs had less complex dendritic trees (n = 10 neurons from 5 mice per group, U = 17156, P < 0.0001, Mann-Whitney test). Scale bar represents 100 μm. Data in **e** are shown as median with shaded interquartile (quartile 1 to quartile 3). (**f**, **g**) In SNI, the iSPN mEPSC frequency was reduced (n = 7 neurons from 5 mice per group; Kolmogorov-Smirnov test for representative cumulative probability plots with D = 0.7491, P < 0.0001; Mann-Whitney test for box plots with U = 8, P = 0.0379). Scale bars represent 20 pA and 400 ms. (**h**) SNI animals had decreased dopamine level in NAc (shown as the percentage of pre-surgery, n = 6 mice per group, U = 2, P = 0.0087, Mann-Whitney test). (**i**, **j**) Medial VTA neurons from SNI had lower firing rates (n = 13 from 6 mice per group, U = 37, P = 0.0140, Mann-Whitney test). Scale bars represent 30 mV and 4 s. Whisker box plots show median, lower and upper quartiles, and whiskers represent minimum and maximum of the data. *P < 0.05, ** P < 0.01.

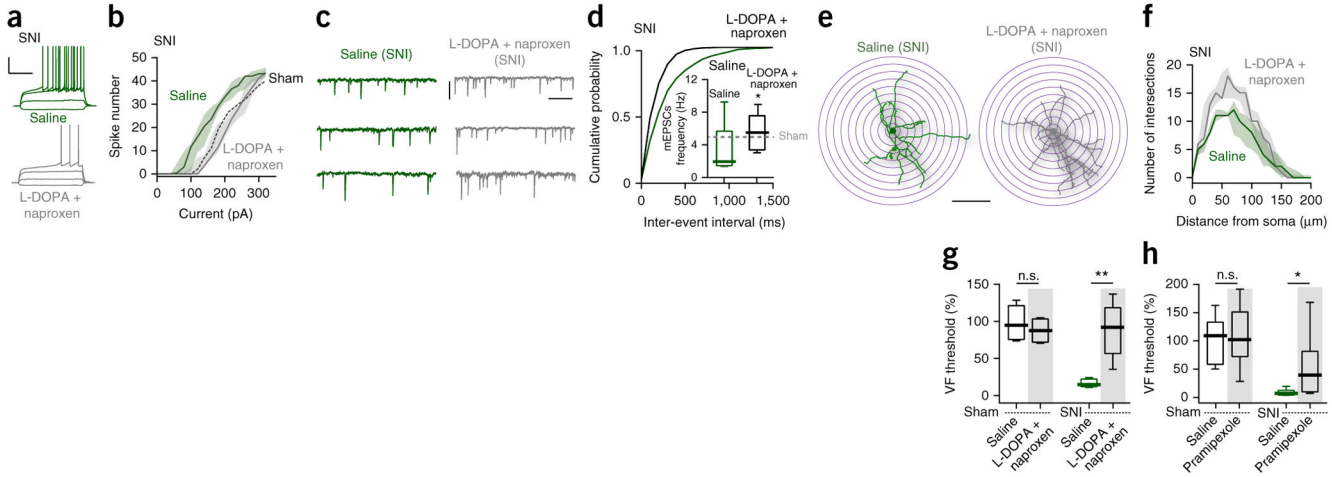

Figure 2.

L-DOPA and naproxen combined treatment prevented SNI-induced reorganization of msNAc iSPNs and blocked tactile allodynia. (**a**–**d**) Combined treatment of SNI animals with L-DOPA and naproxen restored intrinsic excitability (n = 10 neurons from 5 mice per group, U = 11383, P = 0.0006, Mann-Whitney test; **a**, **b**) and synaptic input (n = 8 neurons from 5 mice per group, Kolmogorov-Smirnov test for representative cumulative probability plots with D = 0.2667, P = 0.0097; Mann-Whitney test for box plots with U = 13, P = 0.0499; **c**, **d**). Data in **b** are shown as median with shaded interquartile (quartile 1 to quartile 3). Scale bars represent 30 mV and 300 ms (**a**), and 20 pA and 400 ms (**c**). (**e**, **f**) Combined treatment significantly increased dendritic complexity in iSPNs of SNI animals (n = 7 neurons from 5 mice per group, U = 9149, P = 0.0221, Mann-Whitney test). Data in **f** are shown as median with shaded interquartile (quartile 1 to quartile 3). Scale bar represents 100 μm. (**g**, **h**) Combined treatment (**g**, n = 6 mice for L-DOPA + naproxen-Sham and 5 mice per group for the other 3 groups) or D2 receptor agonist pramipexole alone (**h**, n = 9 mice for pramipexole-Sham, n = 8 for Saline-Sham and Saline-SNI, n = 7 for pramipexole-SNI) blunted tactile allodynia in SNI, but had no effect on tactile response in sham animals (shown as the percentage of pre-surgery; Saline-Sham versus treatment-Sham: U = 10, P = 0.4242, **g**; U = 35, P = 0.9336, **h**; Saline-SNI versus treatment-SNI: U = 0, P = 0.0079, **g**; U = 7, P = 0.014, **h**; Mann-Whitney test). Whisker box plots show median, lower and upper quartiles, and whiskers represent minimum and maximum of the data. n.s., not significant (P > 0.05), *P < 0.05, **P < 0.01.

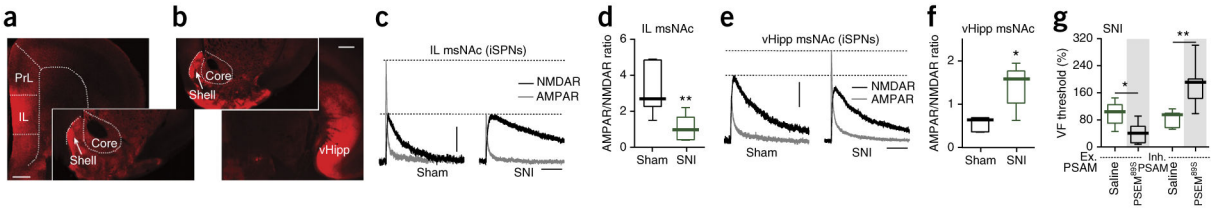

Figure 3.

Excitatory synaptic input to iSPNs was altered by SNI and iSPNs control tactile allodynia. (**a**, **b**) Sample slices displaying the expression of ChR2-mCherry (red) in coronal slices after virus injection in the IL or vHipp. Larger images: virus injection site; smaller images: mCherry-expression in the msNAc. (**a**, IL injections, $n = 12$ paired slices from 10 mice; **b**, vHipp injections, $n = 12$ paired slices from 10 mice). Scale bars represent 0.5 mm. ChR2-mCherry expression was detected at the injection sites and msNAc from all the injected animals. (**c**) Representative AMPAR- and NMDAR-mediated currents elicited at +40 mV in msNAc iSPNs by optical stimulation of IL inputs ($n = 6$ neurons from 5 mice per group). Scale bars represent 50 pA and 100 ms. All SPNs tested had detectable AMPAR and NMDAR currents. (**d**) The IL AMPAR/NMDAR current ratio was reduced by SNI (U = 2, $P = 0.0087$, Mann-Whitney). (**e**) AMPAR and NMDAR currents evoked in NAc iSPNs by vHipp stimulation ($n = 6$ neurons from 5 mice per group) at 3 weeks after ChR2-mCherry virus injection in the vHipp. All SPNs tested had optically evoked AMPAR and NMDAR currents. Scale bars represent 50 pA and 100 ms. (**f**) AMPAR/NMDAR current ratios in NAc shell iSPNs were increased by SNI (U = 3, $P = 0.0152$, Mann-Whitney). (**g**) Intraperitoneal injection of PSEM^{89S} worsened tactile allodynia (percentage of pre-injection) in SNI animals infected with excitatory PSAM (Ex. PSAM: PSAM-5HT3) and blunted tactile allodynia in SNI animals infected with inhibitory PSAM (Inh. PSAM: PSAM-GlyR) (shown as percentage of pre-surgery; $n = 5$ mice in Saline-Ex. PSAM, $n = 6$ in PSEM^{89S}-Ex. PSAM, $n = 7$ in Saline-Inh. PSAM, $n = 7$ in PSEM^{89S}-Inh. PSAM; U = 3, $P = 0.0303$ for Saline-Ex. PSAM versus PSEM^{89S}-Ex.

PSAM; U = 3, $P = 0.0041$ for Saline-Inh. PSAM versus PSEM^{89S}-Inh. PSAM). Data are presented as whisker box plots displaying median, lower and upper quartiles, and whiskers representing minimum and maximum of the data, and analyzed using Mann-Whitney test. $^{*}P < 0.05$, $^{**}P < 0.01$.